2014

Simulation of Model-based Predictive Control Applied to a Solar-assisted Cold Climate Heat Pump System

Jose Candanedo
CanmetENERGY-Varennes, NRCan, Canada, jose.candanedo@usherbrooke.ca

Vahid R. Dehkordi
CanmetENERGY-Varennes, NRCan, Canada, vraissid@NRCan.gc.ca

Simulation of model-based predictive control applied to a solar-assisted cold climate heat pump system

José A. CANDANEDO*, Vahid R. DEHKORDI
CanmetENERGY-Varennes (NRCan), 1615 Lionel-Boulet, Varennes, QC, Canada
Tel.: 450-652-3126 E-mail: jose.candanedo@nrcan.gc.ca

ABSTRACT

This paper presents a simulation study of model-based predictive control (MPC) applied to a heating system using two air-source cold-climate heat pumps. One of the heat pumps uses air preheated by a BIPV/T roof; the other heat pump uses outdoor air. The BIPV/T roof supplying heat to the heat pump has a peak electric output of about 52 kW (out of 104 kW for the entire roof) and covers an area of 320 m^2. A 20-m^3 water tank is used for storing thermal energy supplied by both heat pumps. The paper describes the modelling approaches followed for the building, the heat pumps, the BIPV/T roof and the TES tank. The performance of the system was studied in a Simulink environment. The MPC algorithm was developed in order to select the optimal sequence of operation states for both heat pumps under a time-of-use electricity pricing profile. The MPC algorithm calculates the expected heating load and solves the optimization problem with a genetic algorithm at 24 hour intervals. A comparison of the performance of the MPC algorithm with a benchmark, rule-based control strategy, indicates savings of about 8%.

1. INTRODUCTION

Model-based predictive control (MPC) has received a great deal of attention in recent years as a promising way to improve load management in buildings. MPC also has the potential of improving the performance of building-integrated renewables by making the most of available energy storage capacity to manage the variability of energy generation and utilization. This paper investigates a system with a solar-assisted cold climate heat pump under an MPC strategy, inspired by the design of a net-zero energy commercial building.

3.1 Background and Motivation

In late 2011 and early 2012, CanmetENERGY-Varennes played a consulting role in the design of a net-zero energy library in the municipality of Varennes, near Montreal, Canada. During the design of this library building, with an approximate floor area of 2000 m^2, one of the options considered involved a building-integrated photovoltaic thermal system (BIPV/T) as the main source of heating for a cold-climate heat pump. This BIPV/T-assisted heat pump was to be coupled to a large hot water tank intended as a thermal energy storage (TES) device.

Although the initially proposed BIPV/T-assisted heat pump system was not selected, such a system presented a number of interesting possibilities deserving further investigation. For example, the use of a TES allows new opportunities for load management and dimensioning of HVAC equipment.

Bearing in mind the observations made during the design exercise, it was decided that it was worthwhile to pursue numerical studies on this configuration with the goal of assessing the effect of MPC on the performance of a BIPV/T-assisted heat pump. A model of the system and a reasonable prediction of non-controllable inputs (i.e., weather and occupancy) can be used to implement optimal or near-optimal control sequences in a BIPV/T system with a TES device (J.. Candanedo and Athienitis, 2010; J. Candanedo and Athienitis, 2011).

3.2 Principle of Operation

Building-integrated photovoltaic thermal (BIPV/T) systems and their applications have been widely discussed in the literature (Liao *et al.*, 2007; L. Candanedo, 2010). In essence, a BIPV/T configuration allows recovering thermal energy from PV panels which also play the role as building envelope components (e.g., roof or wall cladding). In the system proposed for the Varennes library, a stream of air moves upwards below the PV modules (Figure 1). Temperature increases of 20-30 °C above the outdoor

temperature have been observed in similar BIPV/T roofs, depending on solar radiation conditions and air flow rates (Doiron, 2011). Such a temperature change indicates that using the BIPV/T air as the source of heat for an air-source heat pump can lead to a significantly better COP.

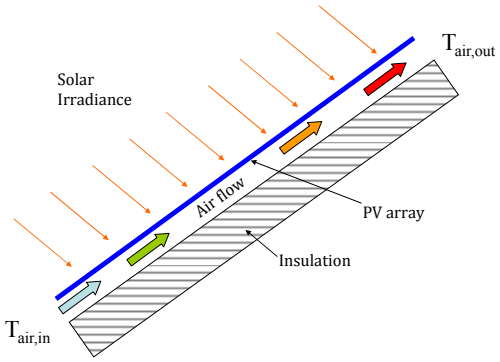

Figure 1: Operation principle of BIPV/T roof

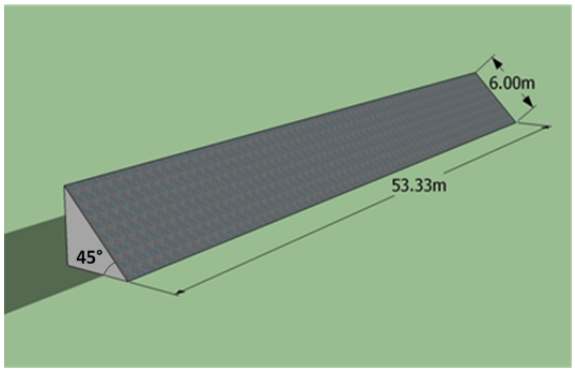

Figure 2: BIPV/T roof geometry in case study building

2. SYSTEM DESCRIPTION

2.1 System Configuration and BIPV/T Roof Features

A south-facing roof section of approximately 53.33 m × 6 m (320 m^2), with a slope of 45°, was made available for a BIPV/T system in the architectural design, corresponding to *half* of the total area covered with PV modules (Figure 2).

Two similar cold climate heat pumps are considered:

- HP1 uses the air heated with the BIPV/T roof;
- HP2, with a nominal heating capacity about twice as large as that of HP1, uses outdoor air.

Heat exchangers supplied by the manufacturer are used to charge a 20 m^3 thermal energy storage water tank. Finally, when required, hot water is diverted to a radiant floor heating system in the building. Figure 3 shows the configuration of the mechanical system proposed.

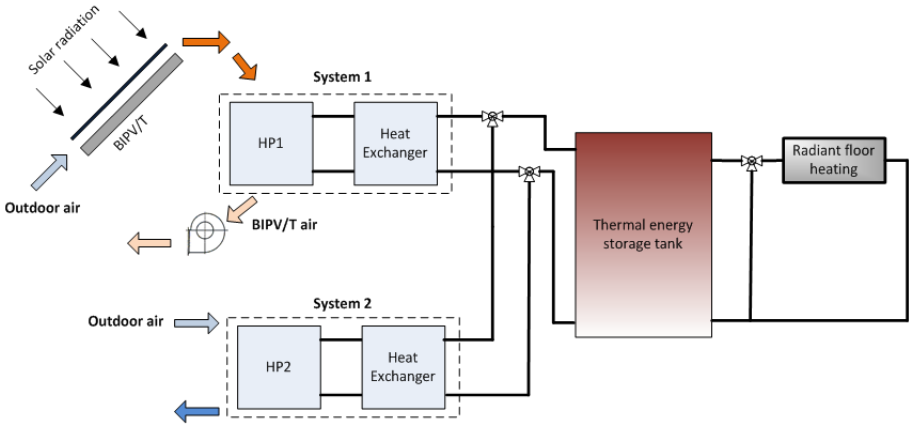

Figure 3: System configuration of BIPV/T-assisted air-source heat pump

The first heat pump system (System 1) is intended mainly to charge the tank when outdoor temperature and solar radiation conditions are favourable (expected BIPV/T temperature above 5 °C). The second heat pump system (System 2) provides heating when the conditions for the operation of HP1 are not favourable.

Table 1 summarizes the most relevant features of the BIPV/T roof, and relevant parameters of the entire system configuration.

Table 1: BIPV/T roof dimensions and parameters

Width of BIPV/T roof	53.3 m
Length of air channel	6 m
Area of BIPV/T roof	320 m^2
Effective area covered by PV	304 m^2 (95%)
Nominal PV efficiency at STC	0.17
Nominal installed capacity in that section	52 kW
Air flow rate in the PV channel	7950 CFM (3750 L/s)
Fan power use	2.25 kW (3 HP)
Thermal energy storage tank size	20 m^3
Roof slope	45°
Gap under roof	6.2 cm
Cross-section of gap	3.30 m^2
Air speed in the channel	1.14 m/s
Roof orientation	Due-south
Temperature coefficient of PV cells	-0.32%/K

3. MODELLING APPROACH

3.1 Simplified Building Model

For the purposes of this investigation, a very simple model was used (2R2C) to mimic the dynamic of the building response. Roughly speaking, node 1 represents the indoor air and the building components not directly linked to the floor (i.e., furniture, inner walls). Node 2 represents the floor and the more massive components receiving solar radiation. In this configuration, it is assumed that 30% of the solar gains are received by node 1 and 70% by node 2. An auxiliary heater (Q_{aux}) delivers thermal energy to node 1 when necessary. Node 2 receives energy from the radiant floor heating system. The RC parameters of the model were obtained by performing an informal calibration to match the annual thermal energy use estimates obtained with other simulation tools (~50,000 kWh/year).

Although quite simple, this model provides a satisfactory representation of the variations of the building heating load, and a coarse approximation of the building time delays.

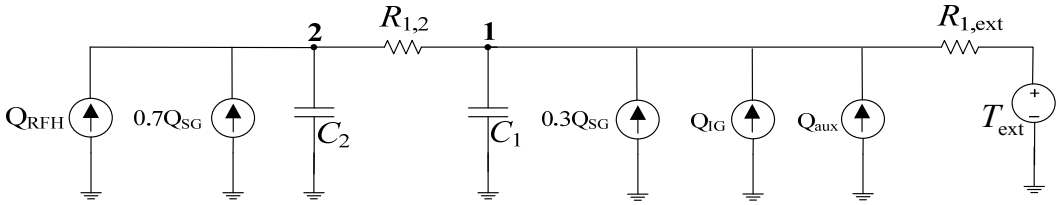

Figure 4: Simplified building model

3.2 BIPV/T Roof Model – Electricity and Heat

In order to model the electricity and heat production of the system, the BIPV/T roof was divided lengthwise in five equally-spaced sections, each 1.2 m long and spanning the whole width of the roof (53.3 m), as shown in Figure 5. It was assumed that the temperatures of the surfaces remain uniform within each control volume. An energy balance was carried out to calculate the temperature of the PV modules, the temperature of the bottom of the channel, the electric power output, the mean temperature of the air within the control volume, and the heat removed by the airstream. After solving the equations within a control volume, the exit temperature of a given section is used as the inlet temperature of the next section. An additional assumption was the utilization of an inlet temperature ($T_{air,in}$) 2 °C higher than the outdoor temperature; this assumption is based on consistent observations in similar installations; this effect is likely based on the heat released by the building façade (Saelens *et al.*, 2004; L. Candanedo *et al.*, 2010).

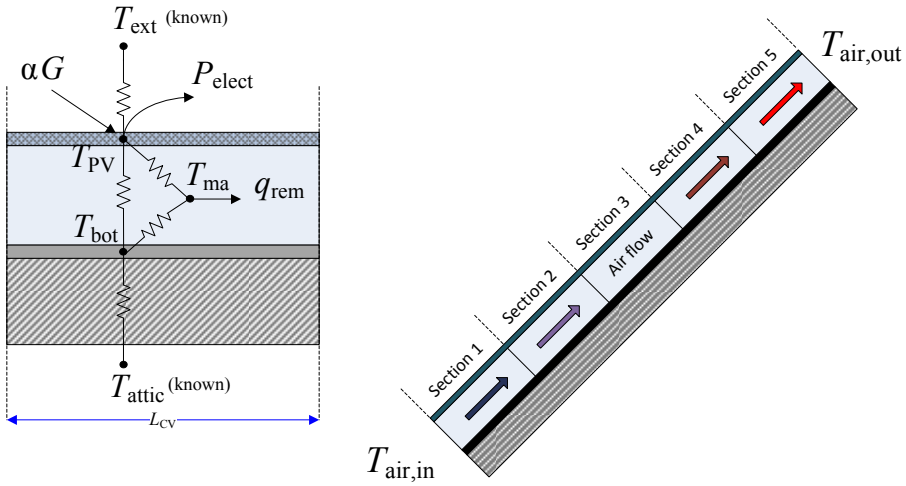

Figure 5: BIPV/T Modelling Approach

The effect of PV temperature on the PV panel efficiency is taken into account with a temperature coefficient of 0.32%/K. For instance, a temperature of 35 °C, 10 °C above standard test conditions, implies a decrease of performance of 3.2%.

$$P_{elect} = P_{STC}\left[1 - 0.0032(T_{PV} - 25°C)\right] \tag{1}$$

The energy balance equations for the three nodes with unknown temperatures (T_{PV}, T_{ma} and T_{bot}) are respectively given by:

$$\alpha G + h_o\left(T_{ext} - T_{PV}\right) + h_r\left(T_{bot} - T_{PV}\right) + h_{ct}\left(T_{ma} - T_{PV}\right) - P_{elect} = 0 \tag{2}$$

$$h_{ct}\left(T_{PV} - T_{ma}\right) + h_{cb}\left(T_{bot} - T_{ma}\right) - q_{rem} = 0 \tag{3}$$

$$h_r\left(T_{PV} - T_{bot}\right) + h_{cb}\left(T_{ma} - T_{bot}\right) + u_{ins}\left(T_{attic} - T_{bot}\right) = 0 \tag{4}$$

In the equations (1) through (4), there are five unknown quantities (P_{elect}, T_{PV}, T_{bot}, T_{ma}, q_{ma}). To complete the set of equations, it can be shown that the mean air temperature (T_{ma}) can be written as a function of the top and bottom temperatures (i.e. T_{PV} and T_{bot}) and the temperature at the entrance of the control volume, T_{in}, which is a known quantity. Defining x as the distance from the beginning of the control volume.

$$T_{ma} = \frac{1}{L_{CV}}\int_0^{L_{CV}} C_1 + \left(T_{in} - C_1\right)e^{-C_2 x}\, dx \tag{5}$$

$$\text{where} \quad C_1 = \frac{h_{ct}T_{PV} + h_{cb}T_{bot}}{h_{ct} + h_{cb}}, \qquad C_2 = \frac{w_{roof}\left(h_{ct} + h_{cb}\right)}{\dot{m}_{air}c_{p,air}}$$

3.3 Group Air-Source Heat Pump + Heat Exchanger

The group "heat pump/heat exchanger" is treated as a single unit. Data obtained from the manufacturer considering the joint operation of both pieces of equipment is used. The original data obtained corresponds to the larger unit (Mitsubishi, 2012). The heat delivery and power consumption of the smaller unit are estimated by dividing by 2. Due to space considerations, the table with the electric energy used by the compressor is not included in this paper.

The MATLAB simulation uses an M-file function with two look-up tables, one for the heat output and one for the electric consumption of the compressor. The operation point is calculated as a function of the temperatures at the source and sink sides of the heat pump (Figure 6). A double interpolation is used for intermediate values.

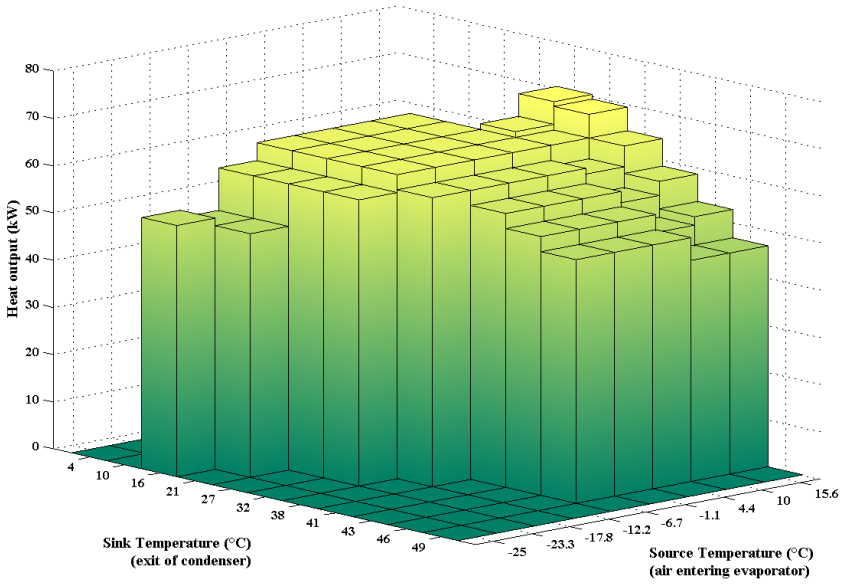

Figure 6: Heat rejected to the condenser in kW_{th} (ΔT = 5.6 °C in the condenser side) for a heat pump/heat exchanger group (model HP192)

Heat pump frost/de-frost cycles was also considered. These cycles depend on the temperature and humidity content of the air in the evaporator side. The frost/defrost cycles were modelled with a MATLAB code containing a table with "correction factors" provided by the manufacturer (Table 2).

Table 2: Correction factors accounting for defrost modes

Inlet wet-bulb air temperature (°C)	6	4	2	1	0	-2	-4	-6	-8	-10	-25
Correction factor	1.00	0.95	0.84	0.83	0.83	0.87	0.90	0.95	0.95	0.95	0.95

It is worth mentioning that the preheating achieved by the BIPV/T roof, due to the corresponding reduction of relative humidity, has the additional benefit of reducing the need to operate in defrost mode.

3.4 Modelling of the TES Tank

In a thermal energy storage (TES) water tank, the colder, denser water drops to the bottom of the tank, while the hotter and less dense water rises to the top. This well-known effect, called thermal stratification, has in general a positive effect in the performance of TES tanks. Hotter water can be taken from the top and used to supply heat to the space, while colder fluid from the bottom facilitates harvesting heat from the source. For this reason, accounting for thermal stratification is important. A very conservative scenario would consist of simulating the tank as a single node, with perfectly mixed water. This assumption would lead to underestimating the system's performance.

The thermal energy storage (TES) tank was modeled with a multi-node approach. This method consists of dividing the tank in a small number of control volumes (Duffie and Beckman, 2006). The fluid entering the tank (in this case, the return water from the radiant floor heating system and the water leaving the heat pump/heat exchanger group) is mixed with the fluid in different control volumes according to their temperatures. A summary of the algorithm is shown in Figure 7.

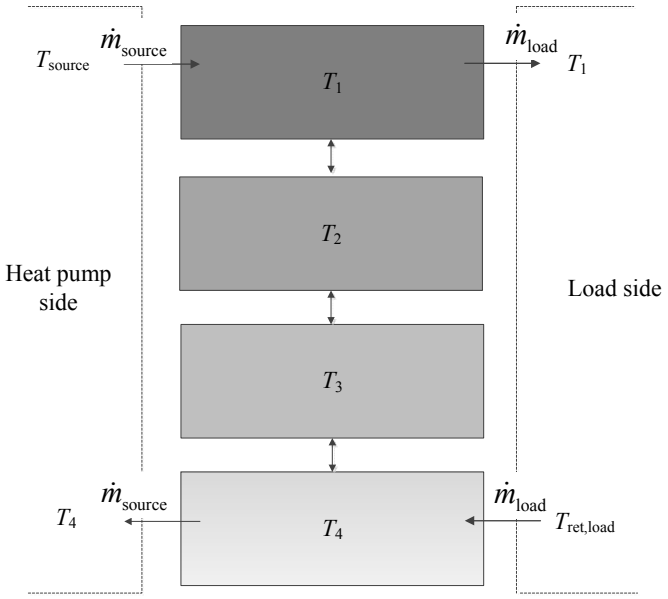

SUMMARY OF ALGORITHM

Flows leaving the tank

- m_{load} times Δt leaves node 1 at T_1
- m_{source} times Δt leaves node 4 at T_4

Flows entering the tank

- IF ($T_{source} > T_2$), then
  - m_{source} times Δt enters node 1 at T_{source}
- ELSE IF ($T_{source} > T_3$), then
  - m_{source} times Δt enters node 2 at T_{source}
- ELSE IF ($T_{source} > T_4$), then
  - m_{source} times Δt enters node 3 at T_{source}
- ELSE IF ($T_{source} <= T_4$), then
  - m_{source} times Δt enters node 4 at T_{source}

A similar approach is used to assign the node for the return fluid from the load.

Flows between nodes

The flowrates between nodes are calculated to comply with conservation of mass. For instance, if node 1 receives 1.5 kg/s from the source and delivers 2 kg/s to the load, then it must withdraw 0.5 kg/s from node 2.

Figure 7: Tank modelling approach.

3.5 Pressure Drop Estimation and Fan Selection

Previous studies (L. Candanedo, 2010) indicate that the pressure drop in a BIPV/T roof cavity can be significantly higher than that of a smooth rectangular smooth channel of the same cross section due to the complex geometry of the cavity. With this estimation, the pressure drop at maximum flow rate is thus roughly 50-70 Pa. However, most of the pressure drop actually occurs in the ducting system. With proper design, the total pressure drop can be reduced to less than 500 Pa. It was estimated that a 3 hp (2.25 kW) fan would be enough to drive a flow rate of 3750 L/s (nearly 8000 CFM) under the BIPV/T roof, based on the following calculation with an efficiency of 85%:

$$P_{fan} = \frac{\dot{V}\Delta P}{\eta}, \quad P_{fan} = \frac{(3.75\ \mathrm{m^3/s})(500\ \mathrm{Pa})}{0.85} = 2.2\ \mathrm{kW} \tag{6}$$

4. Control Algorithms

4.1 Benchmark Strategy

The heating needs of the building are calculated at every time step with a constant indoor set-point of 23 °C and a PID controller for local temperature control. The benchmark control algorithm selects either system 1 (BIPV/T + HP1) or system 2 (HP2 + outdoor air) according to a set of heuristic rules.

- System 1 is used if:
  - It is daytime (between 8:00 and 17:00), *and*
  - TES tank temperatures are acceptable (T_{top} > 30 °C and T_{bot} > 25 °C). Under these conditions, charging the tank can be done at a "normal" pace.
- System 2 is used if:
  - TES tank temperatures are below the acceptable limits described above; (i.e., the tank is discharged and requires urgent charging), *and*
  - Heating is required (the heating load is > 0).
- If the heat pumps do not suffice to provide enough heating to maintain the temperatures in the tank, an auxiliary electric heater is used to heat the space as long as T_{air} < 22 °C and T_{top} < 35 °C.

4.2 MPC Algorithm

The MPC strategy aims to select the combination of System 1 and System 2 that will minimize the operation cost, based on knowledge of the system and weather forecast. For the sake of simplicity, only the electric energy consumption of the heat pumps, the fan and an auxiliary heating system are considered. The MPC algorithm investigated here examines three variables: (a) the state (ON/OFF) of the BIPV/T-assisted heat pump ($\mathbf{x}_{HP\text{-}1}$)*; (b) the state (ON/OFF) of the second heat pump system ($\mathbf{x}_{HP\text{-}2}$); (c) the state of charge of the TES tank ($\mathbf{x}_{TES}$), given by the temperatures of its control volumes.

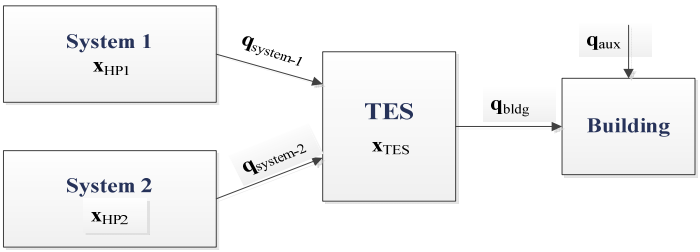

Figure 8: Simplified schematic of system configuration.

The optimization exercise is performed to find the most cost-effective way to supply heating to the building. The cost function is based on a time-of-use (TOU) pricing profile (Figure 9).

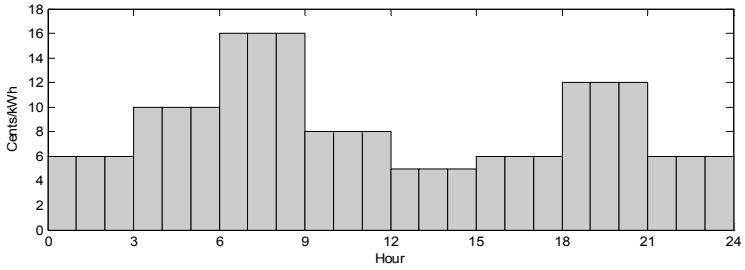

Figure 9: Time-of-use (TOU) pricing profile considered in the optimization.

The objective function is then given by the cost of the electricity use of both heat pumps plus the auxiliary system minus the generation of the entire BIPV/T roof. As shown in Equation (7), an energy cost is only considered when consumption exceeds generation (in other words, no feed-in-tariff is considered).

$$J(\mathbf{x}_{HP\text{-}1}, \mathbf{x}_{HP\text{-}2}) = \sum_{i=1}^{N} C_i \left(P_{Sys1}(i) + P_{Sys2}(i) + q_{aux}(i) - G_{PV}(i) \right) \cdot \left(P_{Sys1}(i) + P_{Sys2}(i) + q_{aux}(i) > G_{PV}(i) \right) \Delta t \quad (7)$$

The complex interaction between the TES tank, the building and the heat pumps is at the core of this optimization problem. The state of operation of each heat pump affects the thermal stratification in the tank, and therefore the energy used by the heat pump in the next time step. The task consists of finding the optimal combination of operation states of the heat pumps (and thus the corresponding temperatures of the control volumes in the tank) that will minimize the cost function over the prediction horizon:

$$\min_{\mathbf{x}_{HP\text{-}1}, \mathbf{x}_{HP\text{-}2}} \quad J\left(\mathbf{x}_{HP\text{-}1}, \mathbf{x}_{HP\text{-}2}\right) \quad (8)$$

$$\text{s.t.} \begin{cases} 21°C < T_{1,air} < 24°C \\ \mathbf{T}_{TES,top} \geq 30\ °C \\ \mathbf{T}_{TES,bot} \geq 25\ °C \end{cases}$$

To simplify the problem, rather than finding the optimal operation states for each hour, the solution is found in 3-hour long periods over a 24-hour control horizon. In other words, the optimization determines the operation of each heat pump in 8 blocks (Figure 10). The solution space for a 24 h period is $4^8 = 65{,}536$.

* The vector notation in bold (e.g., $\mathbf{x}_{HP\text{-}1}$) is used to indicate a sequence of values, e.g. [0 1 1 ··· 0].

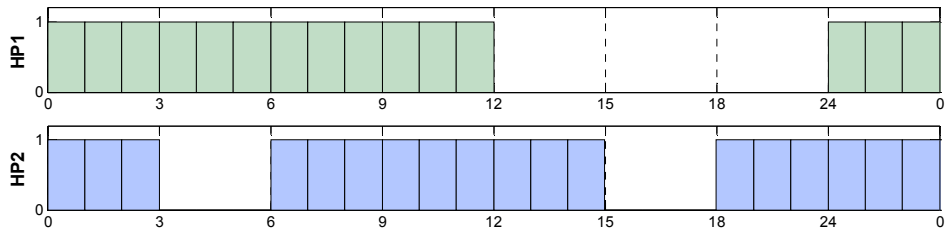

Figure 10: Heat pump operation states in 3-hour blocks - MPC solution for Jan. 14th

A genetic algorithm (MATLAB Global Optimization Toolbox) was used in this study (MATLAB, 2014). Each optimization uses a population of 50 individuals and a maximum of 30 generations. The MPC algorithm can be summarized as follows:

(a) Each day at midnight (0:00), the heating load required to maintain the set-point at exactly 23 °C over the next 24 hours is calculated, given the temperature initial conditions in the building RC circuit and the 4 nodes of the tank. If any cooling is required, an optimization is used to determine the "heating only" profile that will best match the setpoint.

(b) Having the heating load, the genetic algorithm is used to determine the heat pump operation that will satisfy the constraints at the minimum cost over the next 24 hours. Each potential combination of operation states is tested by checking its corresponding effect in the tank temperature, while taking into account the heat withdrawn to satisfy the building load. If required, auxiliary heating is used to maintain the air temperature.

(c) Once the optimal operation states are found, these values are used by the simulation engine. The simulation proceeds until midnight (24:00). The building and the TES states (i.e. temperatures) are updated, and the process is repeated until completing the simulation period of interest.

5. RESULTS AND DISCUSSION

The simulations were carried out in a MATLAB/Simulink environment over the first 15 days of the year. During this period, the median heating load was about 28 kW with a maximum load of 115 kW (the 90th percentile was 50 kW). Results of the benchmark algorithm for a one-week period are shown below (Figure 11). Under the pricing scheme described above, the total cost for the first 15 days of the year is $350.94.

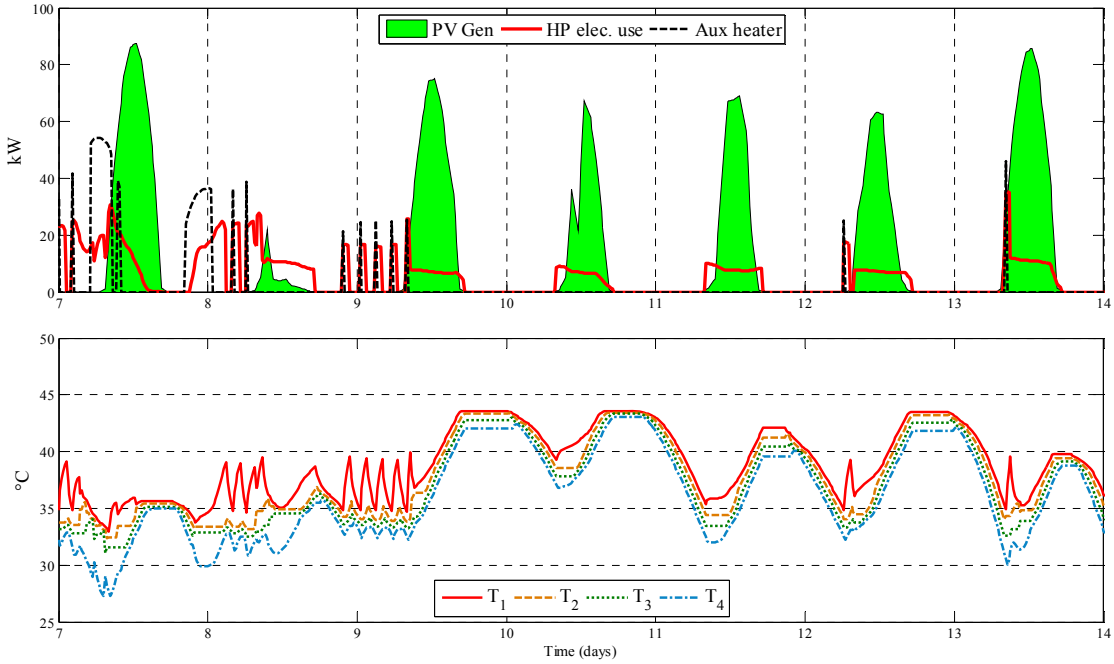

Figure 11: Results of Benchmark algorithm (January 8th to 14th)

The MPC algorithm for the same period yields the results shown in Figure 12. The total cost of the MPC strategy over the first 15 days of the year is $323.39, representing savings of 7.8%. An interesting trend is the fact that the TES tank tends to get charged in anticipation of a high heating demand. The last two days of Figure 12 (starting from t = 12 day) show that the MPC charges the tank in sunny conditions. When heating is required, the TES tank provides heating to the building, while its temperature falls gradually. Unlike the benchmark strategy, no auxiliary heating is required in this period.

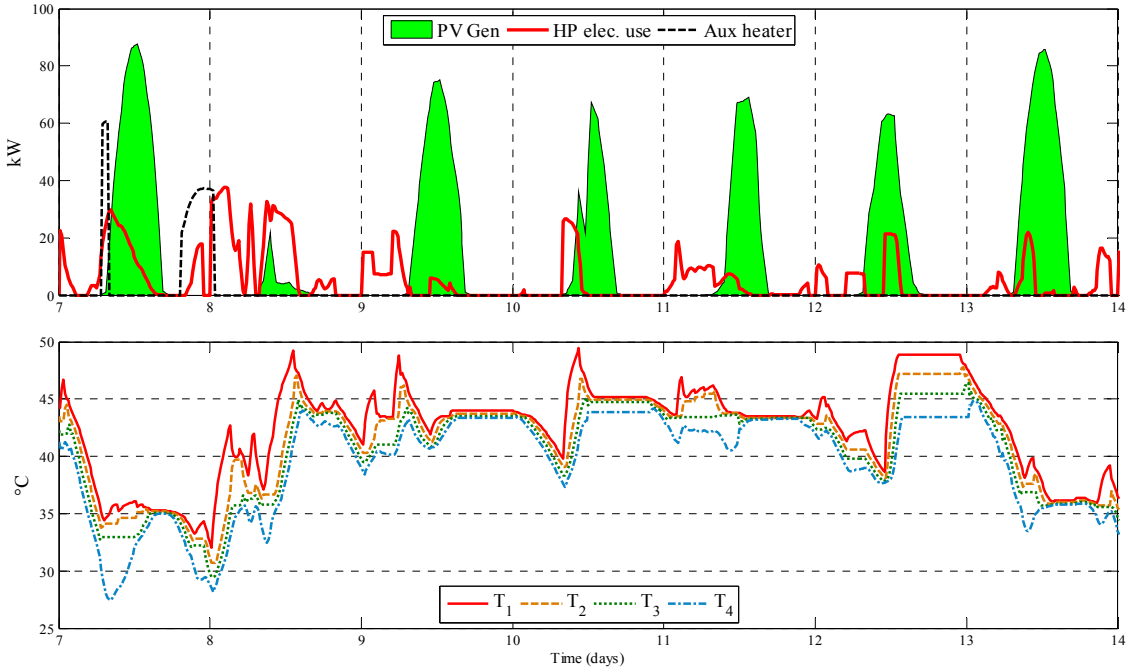

Figure 12: Results of MPC algorithm (January 8th to 14th)

5. CONCLUSIONS

This paper has presented an MPC algorithm applied to a BIPV/T-assisted heat pump for a small commercial building. The incorporation of on-site renewables adds an interesting element, since predictive control can be used to better match local generation with the needs of the building.

The MPC algorithm yields modest benefits (~8%), although these results are strongly dependent on the rate structure. This rate structure will depend on the way the electric utility addresses the building/grid interaction issue. As high peaks of generation or consumption become more problematic, the role of MPC will likely become more significant.

An interesting extension of this work could involve a sensitivity analysis of the effect of the tank size. If the energy storage inventory is too small, then the benefit of anticipatory action are limited. However, beyond a certain size, the benefits of MPC are likely to reach a plateau. Such a sensitivity study could also address building parameters (e.g. effective thermal resistance, thermal capacitance, BIPV/T roof area). It would be interesting to investigate the effect of the prediction horizon (e.g., 48 h instead of 24 h). Finally, the effect of adding uncertainty to the weather forecast and occupancy conditions is worth investigating.

Even when significantly facilitated by the use of models with an appropriate level of resolution, the formulation of an MPC problem can be quite time-consuming and cumbersome. The authors of this study deem that the MPC applications in buildings (at least the first generation) will probably involve the determination of solutions obtained off-line under a set of different scenarios.

NOMENCLATURE

Variables

α	absorptivity of PV modules
G	solar irradiance (Wm^{-2})
P_{elect}	electric power generated (Wm^{-2})
STC	standard test conditions
q_{rem}	heat removed (Wm^{-2})
L_{CV}	length of control volume
u_{ins}	u-value of insulation under channel

		Subscripts	
T	temperature (°C)	air,in	air entering the BIPV/T
		air,out	air leaving the BIPV/T
		ext	outdoor air
		PV	photovoltaic panel
		ma	mean air
		bot	bottom of channel
		attic	attic
		in	inlet of control volume
h	heat transfer coefficient ($Wm^{-2}K^{-1}$)	cb	convective, bottom
		ct	convective, top
		r	radiative (linearized)

REFERENCES

Candanedo, J., Athienitis, A. K., Simplified linear models for predictive control of advanced solar homes with passive and active thermal storage. First High Performance Building Conference, July 12-15 2010 Purdue University, Indiana.

Candanedo, J., Athienitis, A. K., 2011. Predictive control of radiant floor heating and solar-source heat pump operation in a solar house. HVAC & R Research 17(3)**,** pp. 235-256.

Candanedo, L., 2010. Modelling and evaluation of the performance of building-integrated open loop air-based photovoltaic/thermal systems. Ph.D. Thesis, Concordia University.

Candanedo, L., Athienitis, A. K., Candanedo, J., O'Brien, W., Chen, Y., 2010. Transient and steady state models for open-loop air-based BIPV/T systems. ASHRAE Transactions 116(1)**,** pp. 600-612.

Doiron, M., 2011. Whole-building energy analysis and lessons learned for a near net-zero energy solar house. Master's Thesis, Concordia University.

Duffie, J. A., Beckman, W. A., 2006. Solar Engineering of Thermal Processes, Hoboken, New Jersey, John Wiley & Sons.

Liao, L., Athienitis, A. K., Candanedo, L., Park, K. W., Poissant, Y., Collins, M., 2007. Numerical and experimental study of heat transfer in a BIPV/Thermal system. Journal of Solar Energy Engineering 129**,** pp. 423-430.

MATLAB,2014. Global Optimization Toolbox.

Mitsubishi, 2012. PUHY-HP192 Performance Table.

Saelens, D., Roels, S., Hens, H., 2004. The inlet temperature as a boundary condition for multiple-skin façade modelling. Energy and Buildings 36**,** pp. 825-835.

ACKNOWLEDGMENTS

The authors would like to thank Justin Tamasauskas and Jacques Martel for their valuable comments and contributions. The financial support of Natural Resources Canada through the Clean Energy Fund program is gratefully acknowledged.